Published OnlineFirst July 28, 2009; DOI: 10.1158/0008-5472.CAN-09-0301

The Development of a Selective Cyclin-Dependent Kinase Inhibitor That Shows Antitumor Activity

Simak Ali,[1] Dean A. Heathcote,[1] Sebastian H.B. Kroll,[2] Ashutosh S. Jogalekar,[3] Bodo Scheiper,[2] Hetal Patel,[1] Jan Brackow,[2] Alekasandra Siwicka,[2] Matthew J. Fuchter,[2] Manikandan Periyasamy,[1] Robert S. Tolhurst,[1] Seshu K. Kanneganti,[1] James P. Snyder,[3] Dennis C. Liotta,[3] Eric O. Aboagye,[1] Anthony G.M. Barrett,[2] and R. Charles Coombes[1]

Departments of [1]Oncology and [2]Chemistry, Imperial College London, London, United Kingdom and [3]Department of Chemistry, Emory University, Atlanta, Georgia

Abstract

Normal progression through the cell cycle requires the sequential action of cyclin-dependent kinases CDK1, CDK2, CDK4, and CDK6. Direct or indirect deregulation of CDK activity is a feature of almost all cancers and has led to the development of CDK inhibitors as anticancer agents. The CDK-activating kinase (CAK) plays a critical role in regulating cell cycle by mediating the activating phosphorylation of CDK1, CDK2, CDK4, and CDK6. As such, CDK7, which also regulates transcription as part of the TFIIH basal transcription factor, is an attractive target for the development of anticancer drugs. Computer modeling of the CDK7 structure was used to design potential potent CDK7 inhibitors. Here, we show that a pyrazolo[1,5-*a*]pyrimidine–derived compound, BS-181, inhibited CAK activity with an IC_{50} of 21 nmol/L. Testing of other CDKs as well as another 69 kinases showed that BS-181 only inhibited CDK2 at concentrations lower than 1 μmol/L, with CDK2 being inhibited 35-fold less potently (IC_{50} 880 nmol/L) than CDK7. In MCF-7 cells, BS-181 inhibited the phosphorylation of CDK7 substrates, promoted cell cycle arrest and apoptosis to inhibit the growth of cancer cell lines, and showed antitumor effects *in vivo*. The drug was stable *in vivo* with a plasma elimination half-life in mice of 405 minutes after i.p. administration of 10 mg/kg. The same dose of drug inhibited the growth of MCF-7 human xenografts in nude mice. BS-181 therefore provides the first example of a potent and selective CDK7 inhibitor with potential as an anticancer agent. [Cancer Res 2009;69(15):6208–15]

Introduction

Cyclin-dependent kinases (CDK) control cell proliferation by regulating entry into and passage through the cell cycle, initiation of DNA synthesis (S phase), and mitosis (M phase; ref. 1). CDKs are the catalytic subunits of a large family of serine/threonine protein kinases. Activation of specific CDKs is required for the appropriate progression through the cell cycle and into the next stage in the cell cycle. Hence, regulation of CDK activity is pivotal for the correct timing of cell cycle progression and CDK activity is tightly regulated at many levels, including complex formation with cyclins and CDK inhibitors (CDKI) and by phosphorylation and dephosphorylation. Central to the activation of a given CDK is the requirement for association with specific cyclins and phosphorylation at a threonine residue in the activation loop (T-loop; ref. 2). In metazoans, phosphorylation of the CDKs that are required for cell cycle progression (CDK1, CDK2, CDK4, CDK6) is mediated by the CDK-activating kinase (CAK) having three subunits, CDK7, cyclin H (CycH), and MAT1 (3–5).

Deregulation of CDK activity forms an important part of many cancers, as well as other disease states, generally through elevated and/or inappropriate activation, as CDKs are infrequently mutated. Important mechanisms of CDK deregulation include cyclin overexpression, e.g., cyclin D1 (6), and loss of CDKI expression through mutational or epigenetic alterations (for review, see ref. 7). As such, CDKs are important targets for the design of anticancer drugs. Inhibitors of some CDKs, particular emphasis being placed on inhibitors of CDK2 as it controls S-phase entry, have been developed and a few have been tested in the clinical setting as anticancer agents (8–10). One of these is flavopiridol, which has modest selectivity for CDKs over other kinases and inhibits many members of the CDK family (11). The compound class that has yielded many CDK-selective ATP antagonists is 2,6,9-trisubstituted purines, exemplified by roscovitine, which shows good biological and pharmacologic properties (12, 13). CDK7 is an attractive target for drug development due to its critical role in the activation of the CDKs required for cell cycle progression (3, 5). This is especially significant as there is evidence that inhibition of some cell cycle CDKs may be compensated for by other CDKs. Hence, cells from mice that have been ablated for CDK2 are able to cycle, and $CDK2^{-/-}$ mice are viable (14, 15). Similarly, $CDK4^{-/-}$ and $CDK6^{-/-}$ mice are viable, although the double-null mice show late embryonic lethality. However, mice lacking MAT1 die early in embryogenesis (16), indicative of a cellular requirement for CAK. Most described CDK inhibitors that potently inhibit CDK2 also inhibit CDK7, albeit at considerably higher concentrations than the concentrations required for CDK2 inhibition (13, 17). These compounds generally also inhibit other CDKs such as CDK5 and CDK9, which play important roles in neuronal development and transcription (15, 17–19). In addition to its role in cell cycle regulation, CDK7/CycH/MAT1 are components of the general transcription factor TFIIH (20, 21), required for initiation of transcription of RNA polymerase II (PolII)–directed genes. As part of the TFIIH complex, CDK7 phosphorylates the COOH-terminal domain of the largest subunit of RNA polymerase II (3). Further, CAK or TFIIH-associated CAK phosphorylates several transcription factors to regulate their activities (e.g., see refs. 22, 23). Inhibition of CDK7 activity would therefore be expected to inhibit transcription

Note: Supplementary data for this article are available at Cancer Research Online (http://cancerres.aacrjournals.org/).

Requests for reprints: Simak Ali, Department of Oncology, Imperial College London, Hammersmith Hospital Campus, Du Cane Road, London W12 0NN, United Kingdom. Phone: 44-(0)2083833789; Fax: 44-(0)2083835830; E-mail: simak.ali@imperial.ac.uk.

doi:10.1158/0008-5472.CAN-09-0301

Published OnlineFirst July 28, 2009; DOI: 10.1158/0008-5472.CAN-09-0301

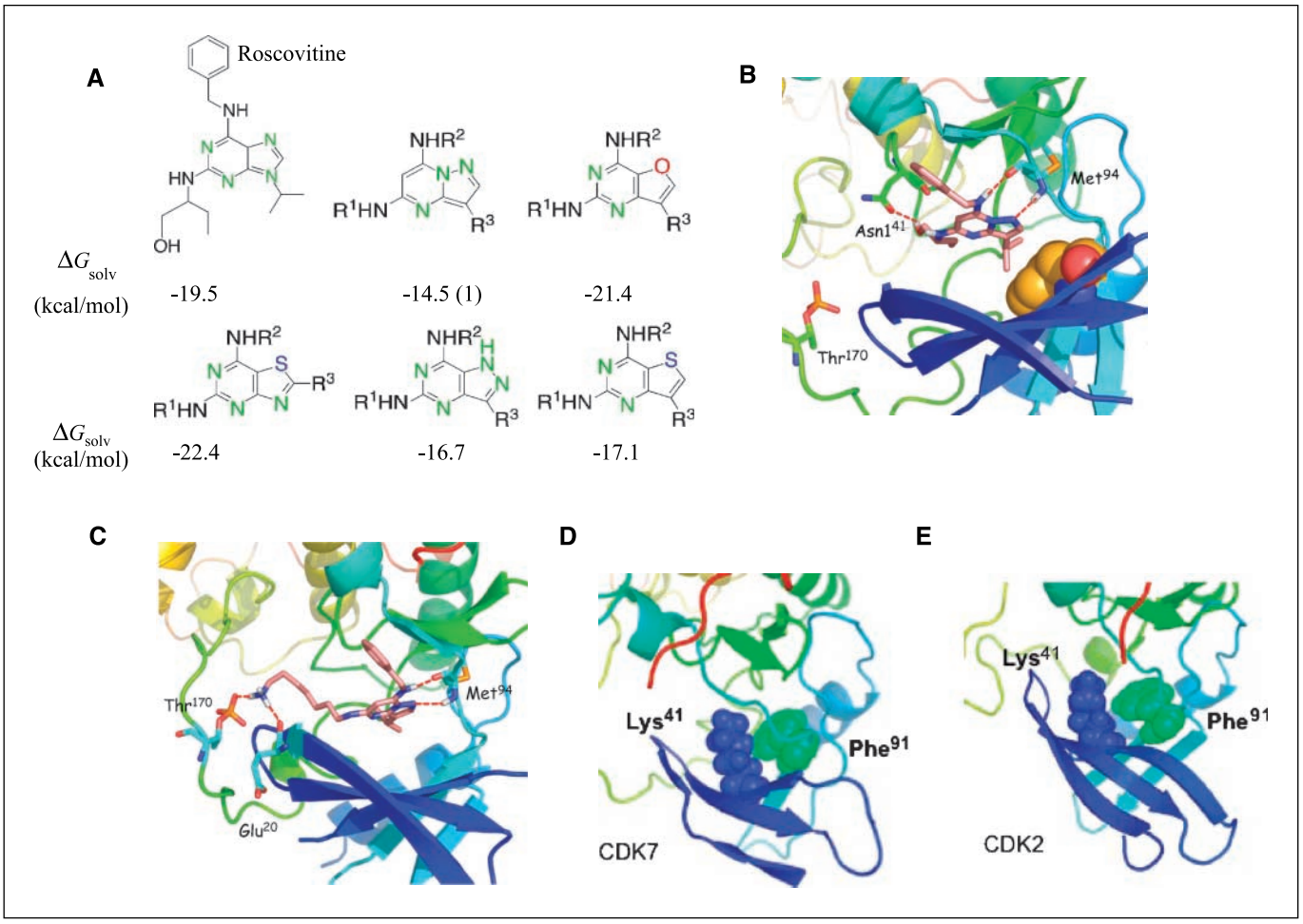

Figure 1. Computational analyses for design of CDK7 Inhibitors. *A,* AMSOL solvation energies of six core motifs based on roscovitine (ΔG_{solv}, kcal/mol). R^1, R^2, and R^3 are the same as those in roscovitine. *B,* lowest energy Glide XP pose for pyrazolopyrimidine **1**. The orange space-filling Phe^{91} is the gatekeeper residue. *Dashed red lines,* hydrogen bonds with Met^{94} and Asn^{141}. *C,* glide XP pose for BS-181 with hydrogen bonds to Glu^{20}, Met^{94}, and Thr^{170} phosphate. Gatekeeper residue packing for CDK7 (*D*) and CDK2 (*E*). The packing is tighter for CDK7 relative to CDK2 as measured by surface exposure of the hydrophobic aggregation of Lys^{41} (*blue*) and Phe^{91} (*green*), 161 and 165 $Å^2$, respectively.

as well as cell cycle progression. Selective inhibitors should therefore provide potentially significant tools for dissecting further the multiple roles of CDK7 and could have utility as anticancer drugs. Here, we have performed computer modeling of the CDK7 structure to identify potential chemical structures that could act as selective CDK7 inhibitors. Based on these analyses, we have identified a novel selective inhibitor of CDK7, named BS-181, which inhibits phosphorylation of CDK7 substrates and inhibits cancer cell growth *in vitro* and *in vivo*.

Materials and Methods

Computer-aided drug design of BS-181. AMSOL v6.6[4] was used to calculate solvation free energies of five preliminary core fragments based on roscovitine. GLIDE (v 4.5) was used to dock the ligands into the CDK7 (PDB ID 1UA2) ATP-binding pocket. All manipulations using GLIDE were performed within the Maestro interface from Schrodinger (v 6.5). The Protein Preparation workflow in Maestro was first used to add protons and assign ionization states to the protein. Following this protocol, a grid centered on the ligand was generated using the default Glide settings. All ligands were docked into this grid structure. Dockings were run using GLIDE SP mode to generate initial poses and then XP and MMGBSA modes to evaluate docking scores and rank ligands with roscovitine as a reference. Ten poses were generated for each docking run and the top pose was picked for evaluation.

General synthetic methods. All manipulations of air- or moisture-sensitive materials were carried out in oven- or flame-dried glassware under an inert atmosphere of nitrogen or argon. Syringes, which were used to transfer reagents and solvents, were purged with nitrogen before use. Reaction solvents were distilled from CaH_2 (dichloromethane, toluene, triethylamine), Na/Ph_2CO (tetrahydrofuran, diethyl ether), or obtained as dry or anhydrous from Aldrich Chemical Company (*N*, *N*-dimethylformamide, acetonitrile) or BDH (ethanol). Other solvents and all reagents were obtained from commercial suppliers (Fluka, Aldrich Chemical Company, and Lancaster Chemicals) and were used as obtained if purity was >98%. All flash column chromatography experiments were carried out on BDH silica gel 60, particle size 0.040 to 0.063 mm, unless otherwise stated. TLC was performed on precoated aluminum-backed or glass-backed plates (Merck Kieselgel 60 F_{254}) and visualized with UV light (254 nm) or potassium permanganate ($KMnO_4$), vanillin or phosphomolybdic acid stains as deemed appropriate. Details

[4] http://comp.chem.umn.edu/amsol

Published OnlineFirst July 28, 2009; DOI: 10.1158/0008-5472.CAN-09-0301

of the synthesis of BS-181 are shown in Supplementary Fig. S1 and in Supplementary Data.

***In vitro* kinase assays.** The purified recombinant CDK2/cycE, CDK4/cycD1, CDK5/p35NCK, CDK7/CycH/MAT1, and CDK9/CycT were purchased from Proqinase GmbH. Kinase assays were performed according to manufacturer's protocols, using substrate peptides purchased from Proqinase GmbH, as described below. A luciferase assay (PKLight assay; Cambrex) was used to determine ATP remaining at the end of the kinase reaction, which provides a measure of kinase activity, according to the manufacturer's protocols.

Cell growth assays. All cells were purchased from the American Type Culture Collection and were routinely cultured in DMEM supplemented with 10% FCS (First Link). Cell growth was assessed using the sulforhodamine B assay, as described (24).

Flow cytometry. MCF-7 cells were seeded (4×10^5) in six-well plates in DMEM containing 10% FCS and allowed to adhere for 24 h, followed by addition of compounds or DMSO and incubation for 24 h. Cells were trypsinized, centrifuged at 1,100 rpm for 5 min, and resuspended in 5 mL of ice-cold PBS, centrifuged as above, gently resuspended in 1 mL ice-cold 70% ethanol, and incubated at 4°C for 1 h. Cells were washed twice with 5 mL of ice-cold PBS and resuspended in 100 μL of PBS containing 100 μg/mL RNase (Sigma-Aldrich) and 1 mL of 50 μg/mL propidium iodide (Sigma-Aldrich) in PBS. Following incubation overnight in the dark at 4°C and filtering through 70-μm muslin gauze into fluorescence-activated cell sorting tubes (Becton Dickinson) to remove cell clumps, stained cells were acquired using the RXP cytomics software on a Beckman Coulter Elite ESP (Beckman Coulter, High Wycombe) and data were analyzed using Flow Jo v7.2.5 (Tree Star, Inc.). For dual labeling with propidium iodide and Annexin V, the cells were trypsinized and collected with the culture medium, centrifuged at 1,100 rpm for 5 min, and washed twice with 5 mL of ice-cold PBS containing 2% (w/v) bovine serum albumin (Sigma-Aldrich). Cells were labeled with Annexin V-FITC using the Annexin V-FITC apoptosis detection kit I (BD Pharmingen), as per the manufacturer's instructions. Labeled cells were acquired within 1 h, by using the RXP cytomics software on a Beckman Coulter Elite ESP, and the data were analyzed using Flow Jo v7.2.5. Statistical analysis was performed for three independent experiments, carried out using the unpaired Student's *t* test to determine *P* values.

Immunoblotting. Cells (1×10^6) were plated in 10-cm plates and were treated with compounds after 24 h. Four hours later, cell lysates were prepared by the addition of 500 μL of hot lysis buffer [4% SDS (w/v), 20% glycerol (v/v), 0.1% bromophenol blue (w/v), 0.1 mol/L Tris-HCl (pH 6.8), 0.2 mol/L DTT, in H_2O], preheated to 100°C. Immunoblotting was performed as described previously (25), using antibodies for PolII (N-20; Santa Cruz Biotechnologies), PolII phosphoserine-2, PolII phosphoserine-5, Rb phosphoserine-795, CDK7, cyclin D1, XIAP, Bcl2, and β-actin from Abcam plc. Antibodies for Rb, CDK2, CDK4, CDK5, cyclin A, cyclin B, cyclin E, and Bcl-xL were purchased from New England Biolabs.

Human tumor xenografts. Seven-week-old female nu/nu-BALB/c athymic nude mice were purchased from Harlan Olac Ltd. All procedures were approved by the CBS, Imperial College London Ethics Committee, and were covered by a Government Home Office project license. Before inoculation of animal with cells, a 0.72-mg 17β-estradiol 60-d release pellet was implanted s.c. (Innovative Research of America). MCF-7 cells (5×10^6) were injected s.c. in not more than 0.1 mL volume into the flank of the animals. Tumor measurements were performed twice per week, and volumes were calculated using the formula 1/2 [length (mm)] × [width (mm)]^2. The animals were randomized and when tumors had reached a volume of 100 to 200 mm^3, animals were entered into the different treatment groups, and treatment with test drug or vehicle control was initiated. Animals were treated with compound twice daily by i.p. injection for a total of 14 d. The compounds were prepared in the vehicle of 10% DMSO/50 mmol/L HCl/5% Tween 20/85% saline. Control mice were injected with the vehicle. Compounds were administered by exact body weight, with the injection volume being not more than 0.2 mL. At the end of the 14-d treatment period, the mice were sacrificed. Throughout the 14-d treatment period, animal weights were determined each day and tumor volumes were determined on alternate days.

Results

Computer-aided drug design approach for the development of potential CDK7 inhibitors. To design CDK7 inhibitors, computational analysis for selection of an alternative core heterocyclic ring structure able to preserve side chain functionality of roscovitine, offer synthetic access, and incorporate suitable solubility properties was carried out. Five motifs (Fig. 1*A*) were evaluated using Amsol 6.6, with the expectation that the structure with the least favorable aqueous solvation energy would be transferred most readily into the hydrophobic kinase active site pocket. The calculated free energies of solvation suggested that pyrazolopyrimidine **1** would be soluble, but the core structure most readily expelled from the water environment and into the protein. Accordingly, this motif was selected for synthetic modification. Docking studies performed using Glide (26, 27) also yielded the best Glide scores for pyrazolopyrimidine **1** compared with the other templates, including roscovitine (Supplementary Table S1).

A key observation in preliminary studies was that **1** with the same side chains as roscovitine docked into the CDK7 active site in the same orientation as the latter, but with slightly better scores and substantially more favorable solvation energies. The best pose for **1** is similar to that for other pyrazolopyrimidines (28). The 3-isopropyl group protrudes into the cavity formed by the gatekeeper Phe^{91}. The N1 and N6 centers form hydrogen bonds with backbone atoms of Met^{94} in the hinge region of the kinase, whereas the side chain hydroxyl makes a hydrogen bond with Asn^{141} (Fig. 1*B*).

The docked pose suggested that **1** is incapable of completely occupying the CDK7 active site pocket. Left unused was a sector in the back of the cleft occupied by two lysines (Lys^{41} and Lys^{138}) and a phosphorylated threonine (Thr^{170}). In an attempt to exploit the lipophilic nature of this subsite, the hydroxy ethyl moiety of **1** borrowed from roscovitine was excised and the resulting propyl side chain was extended. Nonpolar alkyl linkers of different chain length terminating in a variety of polar groups attached to the NH at the C2 position were conceived and docked. A six-carbon linker with a primary amine terminus (Fig. 1*C*) delivered the best docking score and suggested a considerable affinity improvement relative to roscovitine. At the same time, the corresponding Glide pose was similar to that for **1**. In addition to hydrogen bonds in the hinge region, the protonated distal amine was predicted to participate in

Table 1. Inhibition of cyclin-dependent protein kinase activity by BS-181

Kinase	Roscovitine IC_{50}, μmol/L (SD)	BS-181 IC_{50}, μmol/L (SD)
CDK7	0.51 (0.1)	0.021 (0.002)
CDK1	1.8 (0.3)	8.1 (0.6)
CDK2	0.1 (0.02)	0.88 (0.08)
CDK4	15.3 (6.6)	33 (1.5)
CDK5	0.24 (0.1)	3.0 (0.5)
CDK6	28 (4.9)	47 (4)
CDK9	1.2 (0.8)	4.2 (0.5)

NOTE: The mean IC_{50} values (μmol/L) for roscovitine and BS-181, obtained from three experiments, are shown together with the SD from the mean. The line graphs from which IC_{50} values were obtained are shown in Supplementary Fig. S2.

Published OnlineFirst July 28, 2009; DOI: 10.1158/0008-5472.CAN-09-0301

Table 2. *In vitro* growth inhibitory activity of BS-181

Cell type	Cell line	Roscovitine IC_{50}, μmol/L (SD)	BS-181 IC_{50}, μmol/L (SD)
Breast	MCF-7	13 (1.0)	20 (0.5)
	MDA-MB-231	18 (1.0)	15 (0.8)
	T47D	25 (6.5)	16.5 (4.0)
	ZR-75-1	33.5 (2.0)	25.5 (1.3)
	BT474	30.5 (1.0)	30.5 (0.5)
	BT20	32.5 (1.25)	19 (1.25)
	MCF-10A	12.5 (2.3)	15 (1.8)
	HMEC	20.5 (1.3)	17.3 (2.3)
Colorectal	COLO-205	8.0 (3.2)	11.5 (1.5)
	HCT-116	17.5 (1.3)	15.3 (3.8)
	HCT-116 (p53−/−)	8 (2.8)	12.5 (1.5)
Lung	A549	17 (0.8)	37 (3.3)
	NCI-460	9.5 (1.2)	21 (2.0)
Osteosarcoma	U2OS	10.5 (1.0)	14.5 (1.2)
	SaOS2	13.9 (1.0)	20 (1.3)
Prostate	PC3	10.8 (0.3)	18.2 (2.0)
	LNCaP	8.4 (0.3)	24 (0.7)
Liver	HepG2	12.3 (1.0)	15.1 (0.1)

NOTE: The mean IC_{50} values (μmol/L) were obtained using the sulforhodamine B assay. Shown are the mean values derived from at least three replicates, together with the SDs from the means.

strong electrostatic interactions with the phosphate group of Thr^{170} and the backbone carbonyl of Glu^{20}. Simultaneously, the six-carbon linker exhibited productive van der Waals contacts with the floor of the kinase binding pocket (Fig. 1*C*). The same structure was estimated to possess a favorable solvation energy.

Additional docking studies also indicated the structure to favor CDK7 relative to CDK2 (PDB ID: 1B38), CDK5 (PDB ID: 1UNL), and CDK6 (PDB ID: 1XO2), suggesting possible selectivity (Supplementary Table S2). The relative docking scores were confirmed by induced-fit docking.

Synthesis of BS-181 and *in vitro* kinase inhibition. BS-181 was synthesized from dichloropyrazolo[1,5-*a*]pyrimidine **2** (29) by sequential selective substitution of the C-7 chloride using benzylamine, Boc protection, palladium-catalyzed displacement of the C-5 chloride using di-Boc-1,6-hexanediamine under Buchwald-Hartwig reaction conditions (30), and deprotection in acidic methanol (Supplementary Fig. S1). Inhibition of CDK7 activity was measured by incubation of increasing amounts of BS-181 with purified recombinant CDK7/CycH/MAT1 complex, followed by measurement of free ATP remaining in the reaction using a luciferase assay (PKLight, Cambrex), luciferase activity therefore providing a measure of inhibition of CDK7 activity. BS-181 inhibited CDK7 activity with an IC_{50} of 21 nmol/L (Table 1; Supplementary Data Fig. S2), whereas the IC_{50} achieved with roscovitine was 510 nmol/L, in agreement with previous reports for inhibition of CDK7 by roscovitine (13). The IC_{50} values for inhibition of CDK1/cycB, CDK4/cycD1, CDK5/p35NCK, CDK6/cycD1, and CDK9/cycT by BS-181 were considerably higher than 1 μmol/L, with inhibition of CDK2/cycE having an IC_{50} of 880 nmol/L, ~40-fold higher than the IC_{50} for CDK7.

Seventy protein kinases from many different classes were tested for inhibition by BS-181. Some inhibition of the activities of several kinases was observed using high concentrations (10 μmol/L) of BS-181 (Supplementary Table S5). Performing IC_{50} measurements for those kinases that showed the greatest inhibition, CDK2/cycA, CK1, and DYRK1A, showed an IC_{50} of 730 nmol/L, 7.36 μmol/L, and 2.3 μmol/L, respectively. These data confirm that BS-181 is a highly selective inhibitor of CDK7 activity.

BS-181 promotes cell cycle arrest and inhibits cancer cell growth. To assess the antiproliferative activity of BS-181, a panel of cell lines representing a range of tumor types, including breast, lung, prostate, and colorectal cancer, were treated with increasing concentrations of BS-181 for 72 hours. Determination of proliferation using the sulforhodamine B assay showed that growth was inhibited for all cell lines tested, with IC_{50} values ranging from 11.5 to 37 μmol/L (Table 2). The growth inhibition observed for BS-181 was similar to that observed for roscovitine, which gave IC_{50} values in the range of 8 to 33.5 μmol/L.

Immunoblotting of whole cell lysates prepared from MCF-7 cells treated with BS-181 showed inhibition of phosphorylation of the RNA polymerase II COOH-terminal domain (CTD) at the well-established CDK7 phosphorylation site, namely serine 5 (P-Ser5; Fig. 2*A*). Densitometric analysis of the immunoblotting results of three independent experiments indicated that the IC_{50} of inhibition of Ser^5 phosphorylation is 9 μmol/L, whereas 50% inhibition of Ser^5 phosphorylation by roscovitine was not reached at 50 μmol/L. Serine 2 in the CTD, which is not believed to be a substrate for CDK7, but is a substrate for CDK9 and can be phosphorylated by CDK2, was inhibited to a greater extent by roscovitine than by BS-181. BS-181 also inhibited RB phosphorylation at Ser^{795} and Ser^{821} with an apparent IC_{50} of 15 μmol/L (Fig. 2*B*), similar to the IC_{50} obtained for P-Ser2 inhibition.

Immunoblotting for CDKs and cyclins following BS-181 or roscovitine treatment for 4 hours showed down-regulation of CDK4 and cyclin D1 (Fig. 2*C*), with levels of the other CDKs and cyclins remaining unaffected. Additionally, levels of the antiapoptotic

Published OnlineFirst July 28, 2009; DOI: 10.1158/0008-5472.CAN-09-0301

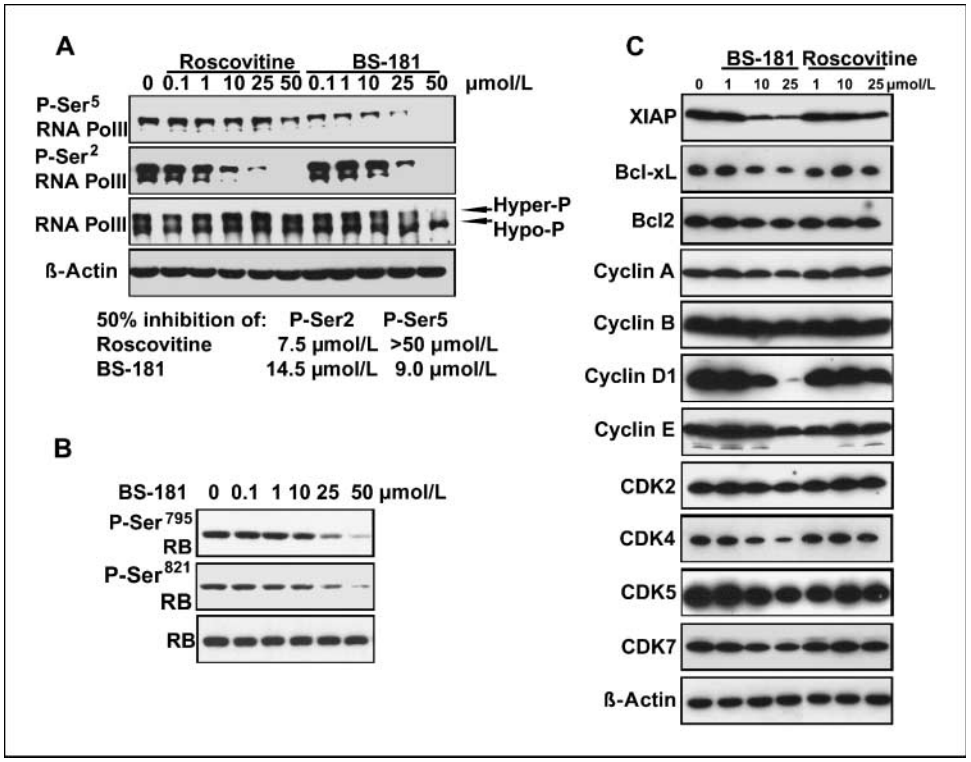

Figure 2. BS-181 inhibits phosphorylation of CDK7 substrates. Whole cell lysates were prepared from MCF-7 cells treated with BS-181 or roscovitine for 4 h, at the concentrations shown. *A,* immunoblotting was carried out using antibodies for RNA polymerase II or Pol II phosphorylated at Ser^2 or Ser^5 in the COOH-terminal domain. The concentration at which apparent inhibition of PolII phosphorylation by 50% would be achieved was determined following densitometry of immunoblots from three experiments. *B* and *C,* immunoblotting was carried out as in *A*, using the antibodies as labeled.

proteins XIAP and Bcl-xL was reduced by BS-181, with Bcl-2 levels being unchanged.

Treatment with low concentrations of BS-181 for 24 hours showed an increase in cells in G_1, accompanied by a reduction in cell numbers in S and G_2-M (Fig. 3*A*; Supplementary Fig. S3). At higher concentrations, however, cells accumulated in the sub-G_1, indicative of apoptosis. This was confirmed by Annexin V staining of cells following BS-181 treatment for 24 hours, with 30% and 83% of cells staining positive for Annexin V with 25 and 50 μmol/L BS-181, respectively (Fig. 3*B*). No significant apoptosis was observed for roscovitine.

***In vivo* pharmacokinetic studies and tumor growth inhibition.** The maximum tolerated single dose for BS-181 given i.p. was determined as 30 mg/kg, with 10 and 20 mg/kg being well tolerated (data not shown). For xenograft tumor growth inhibition studies, therefore, the animals were injected i.p. twice daily with 5 or 10 mg/kg, to give total daily doses of 10 or 20 mg/kg over a period of 14 days. Tumor growth was inhibited in a dose-dependent manner, with 25% and 50% reduction in tumor growth, compared with the control group, for 10 and 20 mg/kg/d doses of BS-181, respectively (Fig. 4*A*). At these doses, there was no apparent toxicity, as judged by lack of significant adverse effects on animal weights (Fig. 4*B*).

I.v. and i.p. administration of 10 mg/kg BS-181 showed rapid clearance (Supplementary Data Fig. S4). The terminal half-lives were 405 and 343 minutes for i.p. and i.v. administration, respectively, with the measured plasma concentration at 15 minutes of 1,950 (SE = 203) and 2,530 (SE = 269) ng/mL, respectively, and bioavailability being 37% for i.p. administration of BS-181 (Supplementary Tables S3 and S4).

Discussion

We show here that BS-181 selectively inhibits CDK7 *in vitro* and treatment of MCF-7 cells results in inhibition of phosphorylation of the CDK7 substrate, Ser^5, in the RNA polymerase II CTD. Further, BS-181 inhibits cell proliferation *in vitro* and *in vivo*. Together, these findings indicate that CDK7 is a potential target for cancer therapy.

The modeling predictions were substantiated when BS-181 proved to be a more potent and selective CDK7 inhibitor than roscovitine. For example, as shown here, roscovitine is an inhibitor of CDK2, CDK5, CDK7, and CDK9, with IC_{50} values of 100, 240, 510, and 1,200 nmol/L, respectively. BS-181, on the other hand, exhibits a substantially higher preference for CDK7 with an IC_{50} value of 21 nmol/L. Excellent selectivity against CDK2, CDK5, and CDK9 is shown by high IC_{50} values of 880, 3,000, and 4,200 nmol/L, respectively. BS-181 also fails to block CDK1, CDK4, and CDK6, with IC_{50} values being >5,000 nmol/L. As such, BS-181 is a highly selective CDK inhibitor and is the most potent CDK7 inhibitor described to date.

It is difficult to rationalize computationally the selectivity of BS-181 for CDK7 over CDK2 and CDK5 in terms of specific ligand-protein interactions. However, different packing interactions of the nonpolar isopropyl side chain at C-3 in BS-181 with the amino acids in the kinase pocket may aid in explaining the phenomenon. For example, the 3-isopropyl side chain protrudes into a cavity formed in part by the important gatekeeper residues Phe^{91} and the C4 carbon chain of Lys^{41} in both CDK2 and CDK7. However, the hydrophobic packing of the two residues is much tighter in the case of CDK7 (Fig. 1*D*) than it is in CDK2 (Fig. 1*E*). This volume-based realignment in the gatekeeper sector of the binding site may well exert a subtle effect that influences selectivity.

The first generation of general CDK inhibitors, such as olomoucine, showed activity against CDK1, CDK2, and CDK5. This was followed by the description of compounds such as UCN-01, which although showing antitumor activity showed side effects that limited their use. Other compounds include

Published OnlineFirst July 28, 2009; DOI: 10.1158/0008-5472.CAN-09-0301

flavopiridol, which is moderately selective against CDK4, CDK6, and CDK1, and CINK4, which is active against CDK4 and CDK6. Paullones have also been shown to have good selectivity against CDK1, CDK2, and CDK5. P276-00 is active against CDK9, with some activity against CDK4 and CDK1 (17, 31). It is only recently, however, that the concept of inhibition of transcriptional control by inhibiting CDK7 or CDK9 has gained some popularity. Inhibition of these kinases may be expected to be particularly important for transcripts that have a short half-life. Examples include transcripts for bcl-2, cyclin D, Mcl-1, and other genes involved in cell cycle progression and apoptosis. For example, flavopiridol, the most potent described inhibitor of CDK9, inhibits phosphorylation of the PolII CTD at Ser^2 and Ser^5 (32, 33) and reduces expression of the antiapoptotic *Mcl-1* gene in primary CLL cells (34). Roscovitine has also been shown to inhibit PolII Ser^2 and Ser^5 phosphorylation and roscovitine (Seliciclib) has been evaluated in a phase 1 study (10). This study showed that the dose-limiting toxicity was fatigue, sickness, and hypokalemia and hyponatremia, with some patients showing evidence of renal failure. No responses were seen although disease stabilization was seen in some patients; the compound was insufficiently active and bioavailable to inhibit PolII phosphorylation. Clinical trials in chronic lymphocytic leukemia (CLL), lymphoma, and multiple myeloma are ongoing for flavopiridol; however, several studies have failed to show clinical responses, although more recent studies in CLL are encouraging and suggest that flavopiridol synergizes with other compounds such as imatinib and tumor necrosis factor–inducing compounds in leukemia (for review and references, see ref. 17).

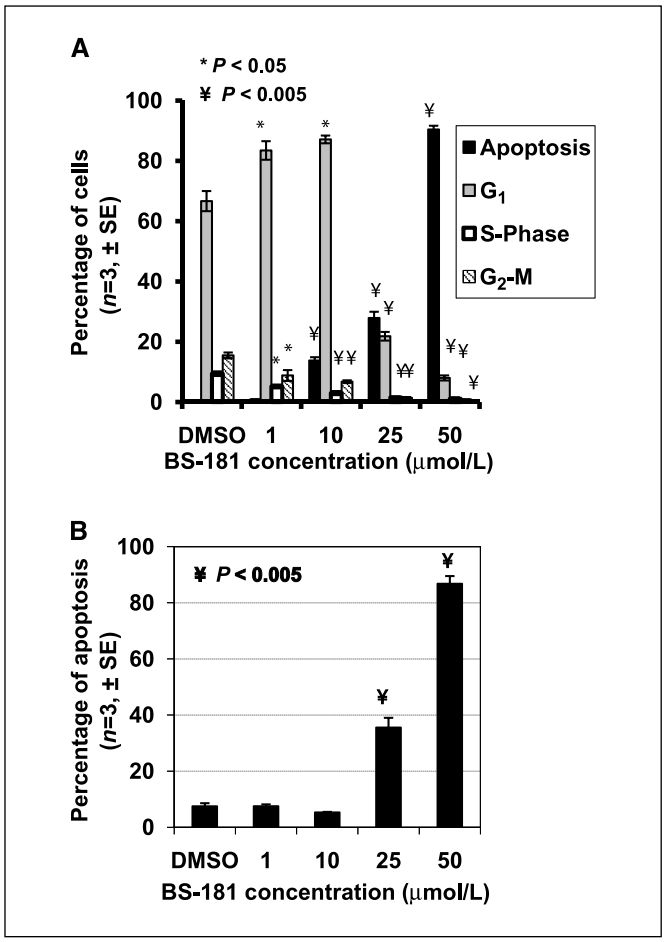

Figure 3. BS-181 treatment of MCF-7 cells leads to G_1 arrest and apoptosis. *A,* MCF-7 cells were treated with BS-181 at the concentrations shown, or with vehicle (DMSO) for 24 h, before fixation, staining with propidium iodide, and flow cytometric analysis. The percentage of cells in the sub-G_1 (apoptosis), G_1, S-phase, and G_2-M, as determined from three independent experiments, are shown. *Error bars,* SE. *B,* cells treated with DMSO or BS-181 were stained with an antibody for Annexin V and with propidium iodide. The percentage of cells that stained positive for Annexin V following the addition of BS-181 or roscovitine are shown for three independent experiments. *Error bars,* SE. *P* values were determined using Student's *t* test, in which comparison between the DMSO control and BS-181 treatment at each concentration was carried out. *, $P < 0.05$; ¥, $P < 0.005$.

BS-181 inhibits phosphorylation of the PolII CTD at Ser^5, a known CDK7 substrate. Although CDK7 does not target Ser^2, BS-181 inhibited Ser^2 phosphorylation, likely through inhibition of CDK2 and CDK9. Indeed, Ser^5 inhibition was observed at lower concentrations of BS-181 than the concentrations required for inhibition of Ser^2 phosphorylation. In this respect, roscovitine, which is a more potent inhibitor of CDK2 and CDK9 than BS-181, inhibited Ser^2 phosphorylation at lower concentrations than BS-181, but only poorly inhibited Ser^5 phosphorylation. Together, these findings suggest that CDK7 is a key target of BS-181 in MCF-7 cells. Inhibition of Rb phosphorylation was also observed, but the inhibition was similar to that observed for Ser^2 of PolII, suggesting that reduction in Rb phosphorylation was indirect.

As outlined above, inhibition of CDK7 and CDK9 has been linked to down-regulation of cyclin D1, bcl-2, and Mcl-1. BS-181 treatment for as little as 4 hours reduced cyclin D1, XIAP, and Bcl-xL expression, although Bcl-2 levels were only slightly reduced. Interestingly, CDK4 levels were also reduced. Together, these data may explain the G_1 arrest and potent apoptosis brought about by BS-181 treatment of MCF-7 cells. Transcriptional inhibitors that block PolII activity, such as α-amanitin and actinomycin D, as well as compounds that inhibit PolII phosphorylation, such as 5,6-dichloro-1-β-D-ribofuranosylbenzimidazole (DRB), have been shown to induce apoptosis by activating p53 (35). Treatment of p53-null HCT116 cells (36) showed considerably reduced, albeit significant, induction of apoptosis by BS-181, compared with p53-positive HCT116 cells (Supplementary Fig. S5), suggesting that p53 is important for BS-181–mediated apoptosis, as described previously for DRB (37). Similarly, greater apoptosis was observed in the p53-positive U2OS osteosarcoma line, when compared with the p53-negative SaOS2 osteosarcoma line (Supplementary Fig. S6). Together, these findings indicate that p53 is important but not essential for BS-181–induced apoptosis.

I.p. injection of BS-181 inhibited MCF-7 tumor xenografts, lending further support to a potential utility of CDK7 inhibitors in cancer treatment. Pharmacokinetic studies showed rapid clearance of BS-181 administered i.p. or i.v. In the case of i.p. administration, the maximal blood concentration of BS-181 was 1,317 ng/mL. Further, bioavailability was only 37%, indicating a need for further refinement of the BS-181 structure to improve stability and bioavailability. As it stands, the studies described here indicate that continuous i.v. infusion or repeated administration is needed for further *in vivo* evaluation. The observed efficacy, despite the low plasma levels (lower than the IC_{50} for growth inhibition *in vitro*), could therefore be due, at least in part, to more active metabolites generated following i.p. administration. Elucidation of the structures of possible metabolites and their activities will be the subject of future studies.

Published OnlineFirst July 28, 2009; DOI: 10.1158/0008-5472.CAN-09-0301

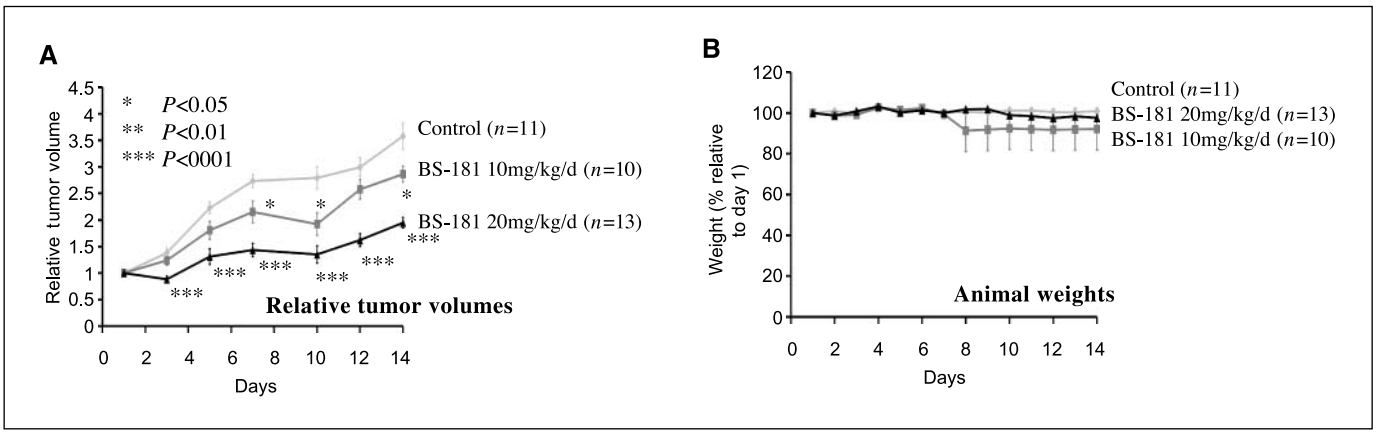

Figure 4. BS-181 inhibits the growth of MCF-7 tumors in nude mice. Randomized MCF-7 tumor-bearing mice were injected i.p. twice daily with 5 or 10 mg/kg BS-181, giving a total daily dose of 10 or 20 mg/kg/d, respectively, over a period of 14 d. Mouse weights were determined daily, tumor volumes being measured every 2 d. *A,* the change in tumor volume was determined for each animal, as tumor volume relative to the tumor volume of each animal at day 1. The line graphs show the mean tumor volumes for the animals in each treatment group. *Error bars,* SE. Asterisks depict the statistical significance of the differences between the control group and each of the BS-181 treatment groups, carried out using Student's *t* test. *B,* animal weights, provided as percentage change relative to the animal weights at day 1. *Error bars,* SE.

In summary, we have discovered the most potent CDK7-selective inhibitor to date by computer-aided drug design. BS-181 selectively exhibited nanomolar enzymatic potency and inhibited all cell lines tested at low micromolar concentrations. For the given route of administration (37% bioavailability), the drug showed *in vivo* activity in human tumor xenografts. BS-181 warrants further preclinical and clinical evaluation as a candidate cancer therapeutic.

Disclosure of Potential Conflicts of Interest

No potential conflicts of interest were disclosed.

Acknowledgments

Received 1/29/09; revised 4/27/09; accepted 5/16/09; published OnlineFirst 7/28/09.

Grant support: Engineering and Physical Sciences Research Council and Cancer Research UK.

The costs of publication of this article were defrayed in part by the payment of page charges. This article must therefore be hereby marked *advertisement* in accordance with 18 U.S.C. Section 1734 solely to indicate this fact.

We thank the Medical Research Council Protein Phosphorylation unit for performing the 70 kinase screening and to Cerep, Inc., for the ADME-Tox and PK studies and Dr. Frances Fuller-Pace for providing the HCT116-p52+/+ and p53−/− lines and for the p53 antibody. We are grateful for support from the NIHR Biomedical Research Centre funding scheme. We also thank the CR-UK and the Department of Health funded Imperial College Experimental Cancer Medicine Centre (ECMC) grant. We wish to dedicate this article to the memory of Dr. David Vigushin, who was instrumental in initiating this project.

References

1. Sherr CJ. Cancer cell cycles. Science 1996;274:1672–7.
2. Morgan DO. Cyclin-dependent kinases: engines, clocks, and microprocessors. Annu Rev Cell Dev Biol 1997;13:261–91.
3. Fisher RP. Secrets of a double agent: CDK7 in cell-cycle control and transcription. J Cell Sci 2005;118:5171–80.
4. Harper JW, Elledge SJ. The role of Cdk7 in CAK function, a retro-retrospective. Genes Dev 1998;12:285–9.
5. Lolli G, Johnson LN. CAK-Cyclin-dependent activating kinase: a key kinase in cell cycle control and a target for drugs? Cell Cycle 2005;4:572–7.
6. Fu M, Wang C, Li Z, Sakamaki T, Pestell RG. Minireview: Cyclin D1: normal and abnormal functions. Endocrinology 2004;145:5439–47.
7. Malumbres M, Barbacid M. To cycle or not to cycle: a critical decision in cancer. Nat Rev Cancer 2001;1:222–31.
8. Knockaert M, Greengard P, Meijer L. Pharmacological inhibitors of cyclin-dependent kinases. Trends Pharmacol Sci 2002;23:417–25.
9. Senderowicz AM. Small-molecule cyclin-dependent kinase modulators. Oncogene 2003;22:6609–20.
10. Benson C, White J, De Bono J, et al. A phase I trial of the selective oral cyclin-dependent kinase inhibitor seliciclib (CYC202; R-Roscovitine), administered twice daily for 7 days every 21 days. Br J Cancer 2007;96:29–37.
11. Losiewicz MD, Carlson BA, Kaur G, Sausville EA, Worland PJ. Potent inhibition of CDC2 kinase activity by the flavonoid L86-8275. Biochem Biophys Res Commun 1994;201:589–95.
12. McClue SJ, Blake D, Clarke R, et al. *In vitro* and *in vivo* antitumor properties of the cyclin dependent kinase inhibitor CYC202 (R-roscovitine). Int J Cancer 2002;102:463–8.
13. Raynaud FI, Whittaker SR, Fischer PM, et al. *In vitro* and *in vivo* pharmacokinetic-pharmacodynamic relationships for the trisubstituted aminopurine cyclin-dependent kinase inhibitors olomoucine, bohemine and CYC202. Clin Cancer Res 2005;11:4875–87.
14. Sherr CJ, Roberts JM. Living with or without cyclins and cyclin-dependent kinases. Genes Dev 2004;18:2699–711.
15. Malumbres M, Barbacid M. Mammalian cyclin-dependent kinases. Trends Biochem Sci 2005;30:630–41.
16. Rossi DJ, Londesborough A, Korsisaari N, et al. Inability to enter S phase and defective RNA polymerase II CTD phosphorylation in mice lacking Mat1. EMBO J 2001;20:2844–56.
17. Shapiro GI. Cyclin-dependent kinase pathways as targets for cancer treatment. J Clin Oncol 2006;24:1770–83.
18. Fischer PM. The use of CDK inhibitors in oncology: a pharmaceutical perspective. Cell Cycle 2004;3:742–6.
19. Pallas M, Verdaguer E, Jorda EG, Jimenez A, Canudas AM, Camins A. Flavopiridol: an antitumor drug with potential application in the treatment of neurodegenerative diseases. Med Hypotheses 2005;64:120–3.
20. Roy R, Adamczewski JP, Seroz T, et al. The MO15 cell cycle kinase is associated with the TFIIH transcription-DNA repair factor. Cell 1994;79:1093–101.
21. Serizawa H, Makela TP, Conaway JW, Conaway RC, Weinberg RA, Young RA. Association of Cdk-activating kinase subunits with transcription factor TFIIH. Nature 1995;374:280–2.
22. Rochette-Egly C, Adam S, Rossignol M, Egly JM, Chambon P. Stimulation of RARα activation function AF-1 through binding to the general transcription factor TFIIH and phosphorylation by CDK7. Cell 1997;90:97–107.
23. Chen D, Riedl T, Washbrook E, et al. Activation of estrogen receptor α by S118 phosphorylation involves a ligand-dependent interaction with TFIIH and participation of CDK7. Mol Cell 2000;6:127–37.
24. Skehan P, Storeng R, Scudiero D, et al. New colorimetric cytotoxicity assay for anticancer-drug screening. J Natl Cancer Inst 1990;82:1107–12.
25. Lopez-Garcia J, Periyasamy M, Thomas RS, et al. ZNF366 is an estrogen receptor corepressor that acts through CtBP and histone deacetylases. Nucleic Acids Res 2006;34:6126–36.
26. Friesner RA, Banks JL, Murphy RB, et al. Glide: a new approach for rapid, accurate docking and scoring. 1. Method and assessment of docking accuracy. J Med Chem 2004;47:1739–49.
27. Friesner RA, Murphy RB, Repasky MP, et al. Extra precision glide: docking and scoring incorporating a model of hydrophobic enclosure for protein-ligand complexes. J Med Chem 2006;49:6177–96.
28. Zhang Y, Li M, Chandrasekaran S, et al. A unique quinolineboronic acid-based supramolecular structure

Published OnlineFirst July 28, 2009; DOI: 10.1158/0008-5472.CAN-09-0301

that relies on double intermolecular B-N bonds for self-assembly in solid state and in solution. Tetrahedron 2007;63:3287–92.
29. Williamson DS, Parratt MJ, Bower JF, et al. Structure-guided design of pyrazolo[1,5-a]pyrimidines as inhibitors of human cyclin-dependent kinase 2. Bioorg Med Chem Lett 2005;15:863–7.
30. Hong Y, Tanoury GJ, Wilkinson CJ, Bakale RP, Wald SA, Senanayake CH. Palladium catalyzed amination of 2-chloro-1,3-azole derivatives: mild entry to potent H-1-antihistaminic norastemizole. Tetrahedron Lett 1997;38:5607–10.
31. Sridhar J, Akula N, Pattabiraman N. Selectivity and potency of cyclin-dependent kinase inhibitors. AAPS J 2006;8:E204–21.
32. Lam LT, Pickeral OK, Peng AC, et al. Genomic-scale measurement of mRNA turnover and the mechanisms of action of the anti-cancer drug flavopiridol. Genome Biol 2001;2:RESEARCH0041.
33. Lu X, Burgan WE, Cerra MA, et al. Transcriptional signature of flavopiridol-induced tumor cell death. Mol Cancer Ther 2004;3:861–72.
34. Chen R, Keating MJ, Gandhi V, Plunkett W. Transcription inhibition by flavopiridol: mechanism of chronic lymphocytic leukemia cell death. Blood 2005;106:2513–9.
35. Gartel AL. Transcriptional inhibitors, p53 and apoptosis. Biochim Biophys Acta 2008;1786:83–6.
36. Bunz F, Fauth C, Speicher MR, et al. Targeted inactivation of p53 in human cells does not result in aneuploidy. Cancer Res 2002;62:1129–33.
37. Gomes NP, Bjerke G, Llorente B, Szostek SA, Emerson BM, Espinosa JM. Gene-specific requirement for P-TEFb activity and RNA polymerase II phosphorylation within the p53 transcriptional program. Genes Dev 2006;20:601–12.

Cancer Research
The Journal of Cancer Research (1916–1930) | The American Journal of Cancer (1931–1940)

AACR American Association for Cancer Research

The Development of a Selective Cyclin-Dependent Kinase Inhibitor That Shows Antitumor Activity

Simak Ali, Dean A. Heathcote, Sebastian H.B. Kroll, et al.

Cancer Res 2009;69:6208-6215. Published OnlineFirst July 28, 2009.